PDG-Arena: An ecophysiological model for characterizing tree-tree interactions in heterogeneous stands

Camille Rouet[a,b,*], Hendrik Davi[a], Arsène Druel[a], Bruno Fady[a], Xavier Morin[c]

[a] *INRAE URFM, Domaine Saint Paul – Site Agroparc, Avignon CEDEX 9, 84914, FRANCE*
[b] *ADEME, 20 avenue du Grésillé, Angers CEDEX 1, 49004, FRANCE*
[c] *CEFE, CNRS, Univ. Montpellier, EPHE, IRD, Montpellier, France, 1919 route de Mende, Montpellier CEDEX 5, 34293, FRANCE*

Abstract

In the context of ongoing climate and biodiversity crises, mixed forest stands are increasingly considered as a sustainable management alternative to monocultures. We developed a new individual-based and process-based forest growth model, PDG-Arena, to simulate mixed forest functioning and test ecophysiological interactions among trees in mixed stands. The model builds upon of a validated ecophysiological stand-scale model and integrates tree competition for light and water. We evaluated the simulation performance of PDG-Arena using annual growth data from 39 common beech and silver fir monospecific and mixed plots in the French Alps. PDG-Arena showed similar performance as the validated stand-scale model when simulating even-age and monospecific forests, and significantly better performance when using structure-diverse and species-diverse inventories. It also showed a significant positive effect of species mixing on gross primary production, canopy absorbance and transpiration. Our results thus show that tree-level process-based models such as PDG-Arena, formally simulating interspecific interactions, are needed to better understand and simulate the functioning of mixed stands.

Keywords: ecophysiology, process-based modeling, mixed forest, competition, biodiversity, overyielding, drought, ray-tracing, French Alps

*Corresponding author
Email address: contact.camille.rouet@pm.me (Camille Rouet)

Contents

1 Introduction 3

2 Materials & Methods 7
2.1 Model description . . . 7
2.1.1 From CASTANEA to PDG-Arena . . . 7
2.1.2 Competition for water . . . 11
2.1.3 Competition for light . . . 12
2.2 Data set . . . 16
2.3 Simulation plan . . . 17
2.4 Model evaluation . . . 18

3 Results 19
3.1 Comparison of the simulation modalities . . . 19
3.2 Modeling performance . . . 19
3.3 Net biodiversity effect . . . 22

4 Discussion 23

5 Declarations 28
5.1 Declaration of competing interest . . . 28
5.2 Funding source . . . 28
5.3 Credits . . . 28
5.4 Author contributions . . . 28

Appendix A Supplementary description of PDG-Arena 29
Appendix A.1 Computing of Leaf Mass per Area . . . 29
Appendix A.2 Estimation of the attenuation coefficient with reverse-engineering . . . 30
Appendix A.3 Distribution of radiations into canopy layers and into sun and shade leaves . . . 33
Appendix A.4 Reduction of absorbed radiations in SamsaraLight . 36

Appendix B Supplementary figures 37

1. Introduction

Understanding how forest ecosystems function is a crucial step for developing forest management strategies adapted to the challenges of global change, particularly climate change (Bonan, 2008; Lindner et al., 2010; Trumbore et al., 2015). In this context, mixed forests, in comparison with monospecific stands, have received increasing attention due to their documented ability to maintain key ecosystem services while enhancing stand resilience (van der Plas et al., 2016; Seynave et al., 2018; Messier et al., 2022; del Río et al., 2022).

However, the physiological functioning of mixed stands is still poorly understood (Forrester, 2014; Forrester and Bauhus, 2016). In particular, if species mixing seems on average to increase stand productivity in comparison to monospecific stands (a phenomenon known as overyielding) (Liang et al., 2016; Zhang et al., 2012; Vilà et al., 2007; Forrester and Bauhus, 2016; Piotto, 2008), this trend depends on stand structure and species composition (Zhang et al., 2012; Ratcliffe et al., 2015), as well as abiotic conditions (Ratcliffe et al., 2016; Toïgo et al., 2015). Regarding the effect of diversity on the resistance of stands to drought episodes, the literature shows heterogeneous results (Grossiord, 2018). Indeed, the direction of the effect seems to depend on the species composition - and particularly on the species respective strategies in reaction to water stress (Pretzsch et al., 2013; Mas et al., 2024; Jourdan et al., 2020) - as well as on environmental conditions (Grossiord et al., 2014; Forrester et al., 2016; Pardos et al., 2021).

Stand structure, particularly tree density and size variability, can act as a confounding factor in the diversity-functioning relationships (Metz et al., 2016; Dănescu et al., 2016; Cordonnier et al., 2019; Zeller and Pretzsch, 2019). To

better understand the processes underlying these relationships, it is therefore important to separate the effects of mixing related to differences in stand structure (age, size, diameter) from those related to differences in the physiological functioning of species (crown architecture, water strategy, nutrient use, etc.) (Forrester and Bauhus, 2016).

Furthermore, the types of interactions observed in a mixture may be of a different nature (Forrester et al., 2016), which could give rise to contradictory effects. For example, an increase in the amount of light captured in mixtures - *e.g.*, through crown complementarity and plasticity, see Jucker et al. (2015) - could lead to an increase in gross primary production, but also in transpiration, with a potentially negative effect on drought resistance (Jucker et al., 2014). Forrester (2014) proposed a conceptual model to account for the mechanisms of interaction between diversity, functioning and environment. In this framework, interspecific interactions resulting in reduced competition for a given type of resource generates beneficial effects for individuals when this resource becomes scarce.

Assessing and predicting the functioning of mixed stands therefore requires detailed knowledge of interspecific interactions. This knowledge must be based on interactions between individuals and on the ecophysiological processes underlying these interactions, i.e. the processes determining competition for light, water and nutrients (Pretzsch et al., 2017; Grossiord, 2018). Furthermore, a detailed understanding of the physiological mechanisms governing the diversity-functioning relationships in forests is all the more necessary as abiotic and biotic conditions, in which tree and species interactions take place, are and will be transformed by global change (Ammer, 2019).

Although experimental and observational systems are necessary for studying the biodiversity-functioning relationship in forests, they are limited by their sample size, measurement completeness and number of confounding factor that can be controlled (Bauhus et al., 2017). Modeling can virtually overcome these limitations, subject to the assumptions contained in the model, which depend to a large extent on our ecological knowledge as well as on the availability of climatic, pedological, silvicultural and physiological data. This approach has been used to put forward hypotheses to explain overyielding in mixing. For example Morin et al. (2011) showed with simulations that overyielding could be explained by the diversity of species traits related to shade-tolerance, maximum height and growth rate (although other explanations were not ruled out). Simulations also make it possible to virtually assess the stability of the productivity of forest mixtures while testing numerous community composition (Morin et al., 2014), even under unprecedented climatic conditions (Jourdan et al., 2021).

The literature (Korzukhin et al., 1996; Cuddington et al., 2013; Morin et al., 2021) depicts a spectrum going from empirical models, based on relationships calibrated from observations between final variables such as productivity and explanatory variables (rainfall, sunshine, etc.), to process-based models whose final variables are computed using explicit elementary processes (photosynthesis, transpiration, phenology, etc.). For some authors (Fontes et al., 2010; Cuddington et al., 2013; Korzukhin et al., 1996), process-based models, because of their supposed greater versatility, seem more relevant for simulating ecosystem functioning undergoing climate change. As a result, they now play an important role in research into the functioning and predicting of forest ecosystem dynamics (Gonçalves et al., 2021). When it comes to simulate mixed stands, models

that simulate elementary processes theoretically have a better ability to reproduce the mechanisms that lead to interspecific interactions, bringing us closer to understanding them (Forrester and Bauhus, 2016).

Among process-based models, a distinction is made between individual-based models, *e.g.* Jonard et al. (2020), and stand-scale models, *e.g.* Dufrêne et al. (2005). Several biodiversity-functioning studies in forests have highlighted the importance of tree-tree interactions in defining the nature of interspecific interactions at the stand level (Trogisch et al., 2021; Jourdan et al., 2020; Guillemot et al., 2020; Jucker et al., 2015). Thus, the individual scale appears relevant for representing the key mechanisms that govern the functioning of mixed forests (Porté and Bartelink, 2002). Finally, process-based and individual-based models have the ability to distinguish the effects of competition between individuals with different functions (mixing effect) and the effects of competition between individuals of different sizes (structure effect). So far, few models are able to simulate mixed stands by taking advantage of both physiological mechanisms and the individual scale (Reyer, 2015; Pretzsch et al., 2015).

Here we present PDG-Arena, a new individual-based, process-based, forest growth model. Our model was developed to observe the stand scale properties that emerge when trees of different species and size compete in a given environment. It was therefore built: (i) from elementary physiological processes using the stand-scale model CASTANEA (Dufrêne et al., 2005) and (ii) by integrating elementary interaction mechanisms among trees, notably competition for light and water. PDG-Arena is designed as an extension of Physio-Demo-Genetics (denoted PDG), a model developed on the Capsis modeling platform (Oddou-Muratorio and Davi, 2014; Dufour-Kowalski et al., 2012).

The performance of PDG-Arena was evaluated using annual growth data from a monitoring network of monospecific and multispecific stands of common beech (*Fagus sylvatica* L.) and silver fir (*Abies alba* Mill.). Firstly, we tested whether PDG-Arena, despite increased complexity, accurately reproduces the performance of CASTANEA when both models are run under comparable conditions. Secondly, we evaluated PDG-Arena's performance in different conditions in terms of stand structure and species diversity. Lastly, using PDG-Arena, we evaluated the net biodiversity effect (i.e. the effect of species mixing) on carbon, light and water processes.

2. Materials & Methods

2.1. Model description

2.1.1. From CASTANEA to PDG-Arena

PDG-Arena was developed as an extension of PDG (Oddou-Muratorio and Davi, 2014) with the aim to simulate the functioning of a diverse, multispecific stand. PDG is an individual-based and spatially explicit model that combines: (1) the process-based model CASTANEA to simulate tree ecophysiological functioning, (2) demographic processes allowing to model tree survival and reproduction and (3) a quantitative genetics simulation module accounting for the heritability and intraspecific diversity of key life history trait of the CASTANEA model. While PDG is built with the idea of simulating the evolutionary dynamic of functional traits, PDG-Arena is designed to simulate ecological interactions between trees.

CASTANEA is an ecophysiological forest growth model that simulates the dynamics of homogeneous stands (Figure 1a). Among others, it has been parameterized and validated on common beech (Fagus sylvatica L., Dufrêne et al.,

2005) and silver fir (Abies alba Mill., Davi and Cailleret, 2017). CASTANEA is composed of five equal-sized leaf layers that perform photosynthesis based on stomatal conductance and on the level of radiation received by each layer, which is determined using a horizontally homogeneous, multi-layer, radiation model. The resulting gross primary production, minus autotrophic respiration, is then allocated into the leaf, fine root, coarse root, branch, trunk and reserves compartments (Davi et al., 2009). The amount of leaf transpiration is determined by net radiation, stomatal conductance as well as ambient temperature and vapor pressure deficit. The stomatal conductance, limiting photosynthesis and transpiration, is controlled by soil water stress. Lastly, leaf phenology is controlled by day length and mean temperature. The temporal scale of the processes in CASTANEA are the same in PDG-Arena, as shown in Table 1.

Table 1: Temporal and spatial scales of physical and physiological processes in PDG-Arena.

	Tree level	**Stand level**
Hourly level	Photosynthesis Respiration Crown transpiration Crown evaporation	Ray casting Soil evaporation
Daily level	Water interception Leaf phenology Carbon allocation	Water balance
Yearly level	Tree growth	

The existing model PDG considers isolated abstract trees, simulating the dynamics of each of them using stand-scale CASTANEA processes. All quantitative physiological variables in CASTANEA and in PDG are related to the stand soil surface: *eg*, the gross primary production is expressed in gC/m^2. The first im-

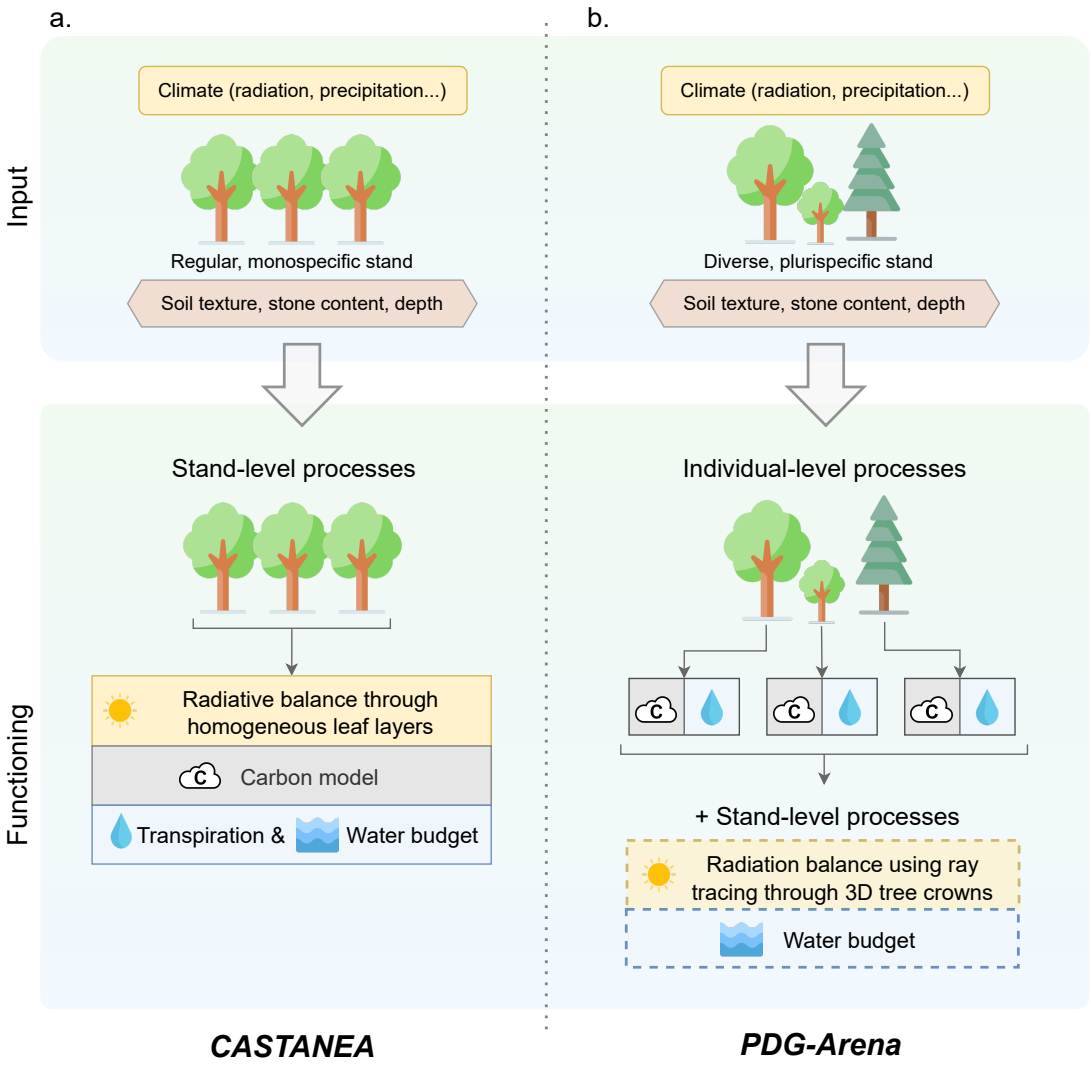

Figure 1: Conceptual diagram of the (a) CASTANEA and (b) PDG-Arena forest growth models input and functioning. CASTANEA simulates the growth of a regular monospecific stand whereas PDG-Arena simulates the dynamics of a diverse multispecific stand. In CASTANEA, all processes, including radiation balance with the SAIL model, carbon fluxes, trees transpiration and soil water budget are held at the stand level, on horizontally homogeneous leaf layers. PDG-Arena takes advantage of CASTANEA carbon and transpiration processes but hold them at the tree level, while a water budget is held at the stand level. The radiative balance is handled by the SamsaraLight library which casts light rays through a 3D representation of a trees crowns. Processes involving competition between trees in PDG-Arena are shown in dashed boxes.

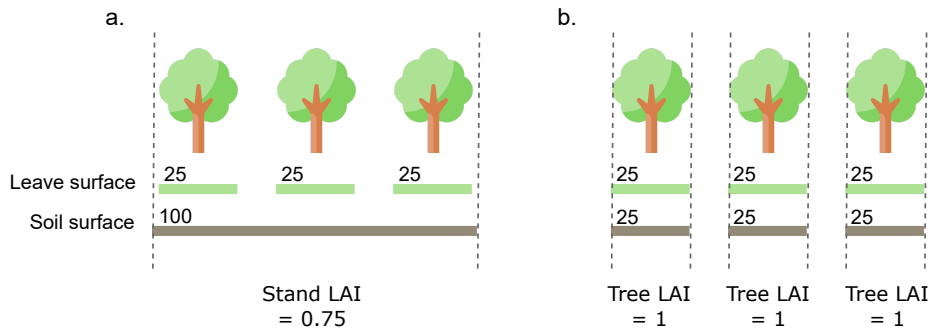

Figure 2: Difference in the representation of Leaf Area Index (LAI) between (a.) the stand-scale model CASTANEA and (b.) the individual-based model PDG-Arena. Values of leaf surface, soil surface and LAI are arbitrary.

provement of PDG-Arena over PDG is that the physiological processes simulate tree functioning instead of stand functioning (Figure 1b). To do so, physiological processes are related to individual trees crown projection surface rather than to the stand soil area. This paradigm shift implied changing the definition of some variables. As depicted in Figure 2, the Leaf Area Index (LAI) is now defined for each tree as the amount of leaf surface of a tree per m^2 of soil under its crown. While the stand LAI in CASTANEA depends on the amount of gap fraction, individual tree LAI in PDG-Arena does not: a tree's LAI only accounts for its leaf surface and its crown projection surface. The same reasoning applies to other physiological variables, such as carbon uptake, water transpiration, absorbed radiation, etc. Also, the Leaf Mass Area (LMA), as it depends on the amount of light intercepted by neighboring trees (Davi et al., 2008a), is computed at the individual level in PDG-Arena according to the vertical profile of the leaf area of neighboring trees (see Appendix A.1).

The second improvement of PDG-Arena over PDG is that it integrates mechanisms of competition for light and water between neighboring trees (see Figure

1b) by: (i) making trees share the same stand soil water pool and (ii) simulating the radiative balance using a ray tracing model.

2.1.2. Competition for water

Competition for water is a crucial element in the water dynamics of mixed stands. We modeled competition for water symmetrically between individuals, i.e., trees in the same plot all draw from the same water reservoir without spatial differentiation, either horizontal (distance between individuals) or vertical (depth). The assumption for no horizontal differentiation is justified here by the small area of the modeled plot.

Every day of simulation, the stand-level volume of precipitation is divided into a portion that does not interact with the canopy – i.e., that falls directly to the ground – and another portion that reaches the canopy. The portion that interacts with the canopy is given by the proportion of soil that is directly under any tree crown. Then, this portion of precipitation is distributed among trees according to their respective leaf surface. For each tree, a calculation of drip, runoff, and precipitation passing through the crown is performed. Transpiration and crown evaporation of trees are calculated individually at the hourly time step using the Penman-Monteith equation (Monteith, 1965), taking into account the energy absorbed by individual crowns (section 2.1.3). Stand soil evaporation is computed at the hourly level and homogeneously along the plot.

Considering drip, runoff and water passing through the crowns on the one hand, and tree transpiration, canopy and soil evaporation and drainage on the other, a water balance is computed at the stand level each day (Table 1 and Figure 1b). Therefore, soil water status (soil moisture, litter moisture and soil potential) is the same for every tree within a plot on any given day.

2.1.3. Competition for light

Competition for light in PDG-Arena is performed using SamsaraLight, a ray tracing library derived from Courbaud et al. (2003) and maintained on the Capsis modeling platform. The integration of SamsaraLight with the physiological model CASTANEA (which is partly inspired from the approach in the HETEROFOR model, Jonard et al., 2020) is described here. PDG-Arena operates two executions of SamsaraLight each year: in the PAR (photosynthetically active radiations) domain and in the NIR (near infrared radiations) domain. For one execution, SamsaraLight generates every year a set of diffuse and direct beams, and computes their interception by tree crowns and soil cells. The simulated energy absorbed by crowns is then temporally distributed at the hourly scale. The energy absorbed by a crown is distributed among its five leaf layers, which are part of a CASTANEA model for each tree.

Definition of crowns.

Each tree is represented by a trunk and a crown occupying a volume in space. Trunks are ignored in the radiation balance, while the characteristics of crowns are defined by the following parameters:

- the height of the tree h;
- its crown base height, hcb;
- its crown radius $crownRadius$;
- its shape, which is considered as conical in the case of Fir and ellipsoidal in the case of Beech (shapes are vertically bounded by h and hcb and horizontally bounded by $crownRadius$);

- its leaf area density at period of full vegetation, denoted LAD, in m^2 of leaf per m^3 of crown volume;
- its attenuation coefficient k;
- its clumping index Ω defining the aggregation of the leaves inside the crown.

Trees h and hcb are inputs of the model (section 2.2). Trees crown radius are determined using an allometric relationship based on species and diameter at breast height (DBH):

$$crownRadius = \beta_{crown} + \alpha_{crown} \times DBH \tag{1}$$

α_{crown} and β_{crown} are species dependent parameters estimated on site at Mont Ventoux (unpublished data from one of the authors, H. Davi). Ω is species dependent and was measured on Mont Ventoux sites by Davi et al. (2008b). The LAD of a tree is the ratio of its maximum leaf area to its crown volume. The leaf area of a given tree i (denoted LA_i) is determined as a portion of its stand leaf area (LA_{stand}). All stand leaf surfaces were measured using Terrestrial Laser Scanning in the summers of 2022 and 2023 (unpublished data from one of the authors, C. Rouet). For every tree, its portion of leaf area is proportionnal to its theoretical leaf area LA_{th}, which is given by an allometric equation based on species and DBH from Forrester et al. (2017b).

The attenuation coefficient k depends on species, radiation domain, type of radiation (direct, diffuse) and beam height angle. Its value is determined using reverse-engineering of SAIL, the radiation sub-model in CASTANEA, as described in Appendix A.2.

Ray casting.

SamsaraLight generates two set of beams. Firstly, diffuse rays are distributed in all the directions at regular interval of 5°. Secondly, direct rays are generated to follow the hourly trajectory of the sun for one virtual day per month. Each set of beams contains the energy of the entire year for both diffuse and direct radiation. The stand plot is subdivided into square cells of 1.5m width. All beams are replicated for each ground cell, aiming at the center of the cell.

Once all the rays have been created, SamsaraLight performs the ray casting as described in Courbaud et al. (2003). For each ray, its energy is attenuated when it crosses an obstacle (in our case, a crown). The proportion of energy transmitted follows the formulation of the Beer-Lambert law:

$$I_T = I_0 e^{-k \times \Omega \times LAD \times l_p} \tag{2}$$

where l_p is the path length of the ray in the crown and I_0 is the energy of the beam before it intercepts the crown. Then, the energy absorbed by a crown I_A is the complement of the transmitted energy:

$$I_A = I_0 - I_T \tag{3}$$

Note that SamsaraLight does not take directly into account the reflection of light - which causes a loss of energy in the sky and a reabsorption of the energy reflected on the ground. These phenomena are taken into account when calculating the attenuation coefficient.

After interception by a crown, the ray continues its course until it reaches either a new crown or a ground cell to which the remaining energy of the ray is

transmitted. At the end of the ray casting, we know for each crown and each soil cell the amount of direct and diffuse energy received in a year.

Computation of hourly absorbed energy.

The hourly absorbed radiation of any element is then computed using the ray casting on the one hand and the hourly incident radiation on the other hand.

For each absorbing element i (a soil cell or a tree crown) and for each type of radiation (direct/diffused, PAR/NIR), the energy it absorbs at the hourly scale is given by the hourly incident radiation $gr(h)$ and the fraction of energy absorbed annually by this element, $I_{Ay}(i)$, divided by the total energy absorbed by all elements j over the year:

$$I_A(h,i) = gr(h) \times \frac{I_{Ay}(i)}{\sum_j I_{Ay}(j)} \tag{4}$$

The value of $I_A(h,i)$ has then to be amended because the ray casting used values of LAD that assume trees were at their period of full vegetation. A surplus of energy is then removed afterward from each tree according to their daily level of leaf development. This surplus is redistributed into other trees and soil cells, as described in Appendix A.4.

Distribution into layers.

Within a real-life tree, some leaves can receive a large amount of light - which leads to a saturation of the photosynthesis capacities - while other leaves are in the shade. The saturation phenomenon (and more generally the concavity of the absorbed light-photosynthesis relation) forbids calculating photosynthesis by considering an average level of light absorption for the whole canopy: this would bias upwards the evaluation of photosynthesis (Leuning et al., 1995). In

CASTANEA, the energy absorbed by the canopy is therefore distributed into five layers of leaves, in which the absorbed energy is assumed to be relatively homogeneous. The layers are themselves divided between leaves in direct light (called sun leaves) and leaves in the shade. The distribution of energy into layers is described in Appendix A.3.

2.2. Data set

The simulations were evaluated at plot scale using dendrochonological data obtained on beech, fir and beech-fir stands from the French pre-Alps (GMAP forest plot design, Jourdan et al., 2019, 2020). The data set includes 39 plots of 10 m radius distributed on three sites (Bauges, Ventoux, Vercors) as described in Table 2, and represents the annual growth dynamics of 1177 stems over the 18-year period 1996-2013. Wood volume increments are obtained by multiplying the individual basal area increments by each tree height. Finally, we used the wood volume increments per stand to evaluate the simulations.

Table 2: Characteristics of the stands used to evaluate the model. Mean value and standard deviation for each site (Bauges, Ventoux, Vercors, all) and composition (Mixed, Beech, Fir, all) are shown for variables: number of stands, altitude (in m), mean diameter at breast height per stand (in cm), density (in stem/ha), basal area (in m^2/ha), proportion of beech basal area (in %), mean age per stand, Leaf Area Index (in m^2/m^2).

Site / Composition	N	altitude	mean DBH	density	basal area	% beech	mean age	LAI
Bauges	10	1100 ± 101	28.7 ± 6.7	1030 ± 685	72 ± 14	0.53 ± 0.43	89 ± 16	3.0 ± 0.4
Vercors	14	1250 ± 101	32.3 ± 8.6	657 ± 275	56 ± 14	0.53 ± 0.38	118 ± 40	3.0 ± 0.8
Ventoux	15	1250 ± 126	22.1 ± 6.3	1450 ± 623	57 ± 13	0.50 ± 0.40	105 ± 47	2.9 ± 0.5
Mixed	13	1200 ± 131	26.2 ± 7.3	1080 ± 465	64 ± 13	0.46 ± 0.10	101 ± 29	2.6 ± 0.5
Beech	14	1230 ± 118	26.7 ± 10.3	1200 ± 794	56 ± 14	0.97 ± 0.05	119 ± 35	3.3 ± 0.6
Fir	12	1190 ± 139	29.8 ± 7.4	867 ± 578	62 ± 18	0.05 ± 0.07	94 ± 50	2.9 ± 0.6
all	39	1210 ± 126	27.5 ± 8.4	850 ± 632	60 ± 15	0.51 ± 0.39	105 ± 39	2.9 ± 0.6

Field inventories include the position, height, crown base height, age, diameter and species of every tree with DBH greater than 7.5 cm in each of the 39 stands. Hourly climate data (temperature, global radiation, wind speed, precipitation and relative humidity) were obtained from the 8 km scale SAFRAN reanalysis dataset (Vidal et al., 2010) for the three sites and temperatures were adapted to each stand altitude using an adjustment of 0.6 °C/100m (Rolland, 2003). Soil texture, depth and stone content were obtained for every stand (unpublished data from one of the authors, X. Morin).

2.3. Simulation plan

Using field inventories, we generated three sets of virtual inventories for PDG-Arena, following three levels of abstraction, denoted RN, RS and O. The first set represents regularized inventories with no species interactions (RN): for each species of each stand, we generated a new inventory with equally spaced trees of the same species, age, diameter and height. The simulation results using regular monospecific inventories generated from the same stand were then assembled relatively to the proportion of each species basal area. RN inventories can then be used to simulate the growth of multispecific stands, ignoring species interactions. The second set represents regularized inventories with species interactions (RS): trees of the same species share the same age, diameter and height. Plus, trees are regularly spaced in a random order, independently of the species. Lastly, original inventories (O) include the information of the real life dataset, that is: species, position, diameter and height of every individual trees. For each type of inventories representing the same stand (regularized or not, with or without species interactions), the mean quadratic diameter, volume per tree and tree age per species and the basal area were conserved.

CASTANEA was used as a reference model to evaluate the performance enhancement brought by PDG-Arena. We used regularized inventories with no species interactions (RN) for CASTANEA's stand-scale simulations. It is to be noted that, contrary to PDG-Arena, CASTANEA does not account for the stand slope. Therefore, when comparing CASTANEA and PDG-Arena results (section 3.1), the slope was put to zero in PDG-Arena inventories. In the other situations (sections 3.2 and 3.3), the slopes of the inventories simulated using PDG-Arena were those of the field data.

To sum up, we simulated the growth of 39 stands over the 18-year period 1996-2013, considering four modeling situations: RN, RS and O inventories with PDG-Arena on the one hand, and RN inventories with CASTANEA on the other hand. Tree reproduction and intraspecific diversity, which are characteristics of PDG and therefore PDG-Arena, were switched off for these simulations. Inventories, simulation results and the analysis script were deposited on the Zenodo repository platform (Rouet, 2024).

2.4. Model evaluation

To evaluate the similarity between each modeling situation, we used the gross primary production (GPP) as CASTANEA and PDG-Arena are carbon-based models. We computed the coefficient of correlation (r, from -1 to 1) for the simulated GPP per stand between the four situations of simulation.

To evaluate the performance of the models against field measurements, we used the simulated wood volume increment per stand. We computed the Mean Absolute Percent Error (MAPE) and the coefficient of determination (r^2, from 0 to 1) between simulations and measurements. A low MAPE indicates that simulated wood production is on average close to measured production. A r^2

close to 1 shows a good capacity of the model to predict the stand production variability.

Lastly, we evaluated the net biodiversity effect (NBE) to informs us about the presence of physiological processes that are caused by species mixing. It is defined as the difference for a variable between its observed value in mixed stands and its predicted value based on the hypothesis that there is no complementarity effect between species (Loreau, 2010). Here, we compared the value of a simulated variable with PDG-Arena using RS and RN inventories. The NBE was evaluated on GPP, canopy absorbance, transpiration rate and water shortage level (defined as the maximum difference reached during simulation between the current and full useful reserve, in mm). The NBE was tested against the null hypothesis using two-sided Wilcoxon signed rank test.

3. Results

3.1. Comparison of the simulation modalities

Using regularized inventories with no species interactions (RN), CASTANEA and PDG-Arena showed similar predictions for the stand-level GPP, as represented in Figure 3. The coefficient of correlation between the two models was estimated at 99.6%. Moreover, as shown in Table 3, which compares the 4 modeling situations based on the coefficient of determination, PDG-Arena was closer to CASTANEA when using regularized stands and when species interactions were disabled.

3.2. Modeling performance

Performances of CASTANEA's and PDG-Arena's simulations against measured wood volume increment per stand are reported in Table 4. Firstly, PDG-

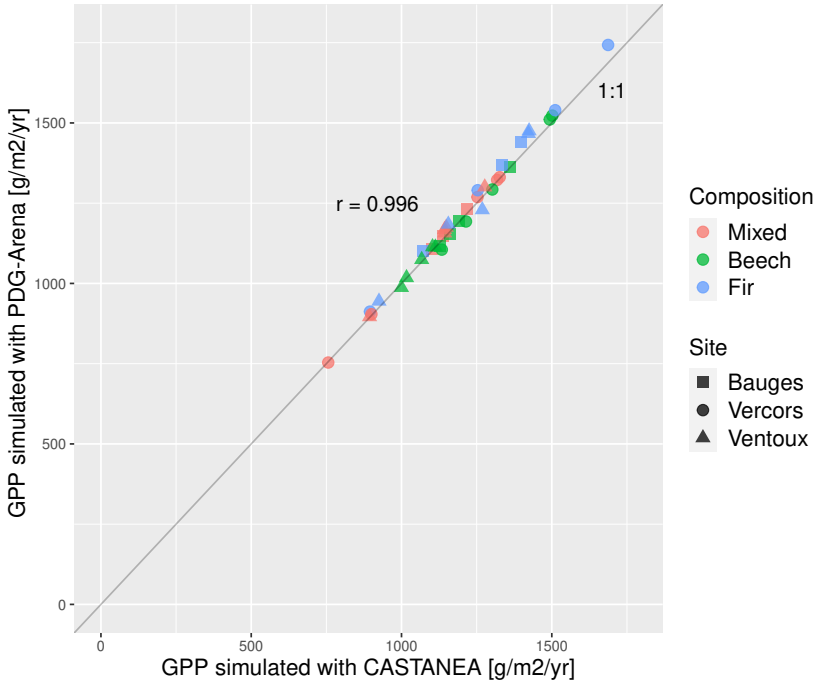

Figure 3: Gross primary production (GPP) per stand simulated by PDG-Arena and CASTANEA. Regularized inventories with no species interactions (RN) were used. r is the correlation coefficient.

Table 3: Matrix of similarity between simulated GPP from CASTANEA and PDG-Arena using different types of inventories: 'RN' (regularized with no species interactions), 'RS' (regularized with species interactions) and 'O' (original inventories). Similarity is expressed using the correlation coefficient (in %) of the simulated gross primary production for the 39 stands over the 1996-2013 period.

	CASTANEA (RN)	PDG-Arena (RN)	PDG-Arena (RS)	PDG-Arena (O)
CASTANEA (RN)	100.0	-	-	-
PDG-Arena (RN)	99.6	100.0	-	-
PDG-Arena (RS)	98.4	99.0	100.0	-
PDG-Arena (O)	96.5	97.4	98.4	100.0

Table 4: Evaluation of the performances of PDG-Arena and CASTANEA. Coefficient of determination (r^2, in %) and Mean Absolute Percent Error (MAPE, in %) were computed for the simulated versus measured yearly wood volume increment per stand over the period 1996-2013. Inventories are characterized as: 'RN' (regularized with no species interactions), 'RS' (regularized with species interactions) and 'O' (original inventories).

Set	Model	Inventories	r^2	MAPE
All stands	CASTANEA	RN	17.6	44.0
	PDG-Arena	RN	18.4	43.0
	PDG-Arena	RS	19.0	43.2
	PDG-Arena	O	20.9	40.5
Mixed	CASTANEA	RN	40.2	36.4
	PDG-Arena	RN	40.3	37.8
	PDG-Arena	RS	43.1	38.9
	PDG-Arena	O	50.1	34.1
Beech pure	CASTANEA	RN	22.0	53.1
	PDG-Arena	RN	21.6	51.6
	PDG-Arena	RS	21.6	51.9
	PDG-Arena	O	36.2	47.0
Fir pure	CASTANEA	RN	7.8	41.5
	PDG-Arena	RN	12.5	38.5
	PDG-Arena	RS	11.5	37.8
	PDG-Arena	O	12.9	40.0

Arena gave slightly better performances than CASTANEA on comparable inventories, i.e. RN inventories (r^2 18.4 vs 17.6%, MAPE 43.0 vs 44.0%). Using the original stand dataset (O), PDG-Arena performed better than CASTANEA (r^2 20.9% vs 17.6%, MAPE 40.5% vs 44.0%), with particularly better predictions for mixed (r^2 50.1 vs 40.2%, MAPE 34.1 vs 36.4%) and beech stands (r^2 36.2 vs 22.0%, MAPE 47.0 vs 53.1%). Both PDG-Arena using O inventories and CASTANEA using RN inventories had poor prediction capacity for the fir stands, although PDG-Arena performed better than CASTANEA (r^2 at 12.9% vs 7.8%). The mean absolute error was larger for beech stands, moderate for fir stands and lower for mixed stands: respectively, 53.1%, 41.5% and 36.4% for CASTANEA and 47.0%, 40.0% and 34.1% for PDG-Arena using O inventories.

Activation of species interactions in PDG-Arena (RS vs RN inventories) enhanced the r^2 on mixed stands (43.1 vs 40.3%) but also slightly increased the mean absolute error (38.9 vs 37.8%). Using original instead of regularized inventories (O vs RS), PDG-Arena gave better performances on mixed (r^2 50.1 vs 43.1%, MAPE 34.1 vs 38.9%) and beech (r^2 36.2 vs 21.6%, MAPE 47.0 vs 51.9%) stands and similar performance on fir stands (r^2 12.9 vs 11.5%, MAPE 40 vs 37.8%).

3.3. Net biodiversity effect

The GPP and canopy absorbance simulated by PDG-Arena in mixed stands are represented in Figure 4 for RN, RS and O inventories. Additionally, Figure B.7 shows the maximum water shortage and yearly transpiration rate. Comparison of simulations with RS and RN inventories showed a positive net biodiversity effect on GPP (1180 vs 1110 gC/m2/year; p-value < 0.001) and canopy absorbance (0.332 vs 0.302; p-value < 0.001), but also on canopy transpiration (171 vs 150

mm; p-value < 0.001) and maximum water shortage (74.8 vs 67.6 mm; p-value < 0.001). The mixing effect, i.e. the fact of simulating species in interaction instead of separately, thus increased the GPP and canopy absorbance of 6.1% and 10.1% respectively, and also increased the transpiration and water shortage of 14.0% and 10.7%, respectively.

The structure effect (evaluated by comparing O and RS inventories on all 39 stands, not shown here) slightly decreased the GPP (1180 vs 1220 gC/m2/year; p-value $< 10^{-4}$) and canopy absorbance (0.316 % vs 0.330%; p-value $< 10^{-4}$). Transpiration also showed a slight decrease (167 vs 172 mm; p-value $< 10^{-4}$) and maximum water shortage showed no significant variation (74.7 vs 75.5 mm; p-value > 0.05).

4. Discussion

Given the paucity of forest growth models simulating ecophysiological processes at the individual scale, we developed the individual-based model PDG-Arena from the stand-scale model CASTANEA in order to simulate mixed forests. PDG-Arena was built with the idea of observing and understanding the properties that emerge in multispecific stands. It uses on the one hand a physiological model parameterized for monospecific stands and on the other hand an individual scale structure that allows trees to interact - the interaction being more of less competitive depending on the functional traits of the individuals and species.

We showed that PDG-Arena was able to reproduce the behavior of CASTANEA when simulating regularized inventories with no species interactions. Thus, the increase in complexity of PDG-Arena, made necessary in order to simulate the functioning and interactions of distinct trees, was not at the cost

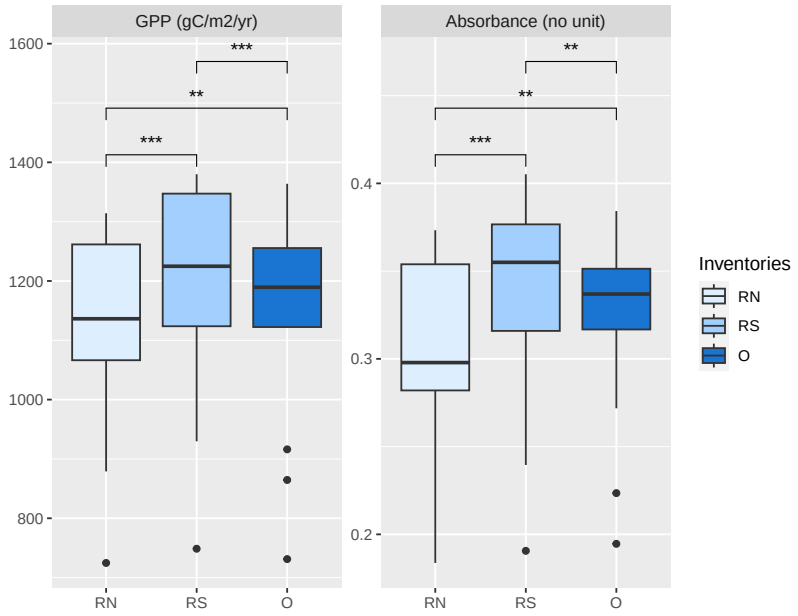

Figure 4: Gross primary production (GPP) and canopy absorbance simulated by PDG-Arena for 13 mixed stands. Three types of inventories were used: regularized inventories with no species interactions (RN), regularized inventories with species interactions (RS) and original inventories (O). Two-sided Wilcoxon signed rank test was used (**: p-value < 0.01, ***: p-value < 0.001).

of decreased performance at the stand scale. PDG-Arena, in comparison to CASTANEA, is able to account for stands' irregular structure and diversity in species and showed better performance, particularly on beech (r^2 +14.2 percentage points) and mixed stands (r^2 +9.9 percentage points). Moreover, as shown by the simulations using different types of inventories, the improvement in simulating stand growth is explained by both the integration of interspecific interactions and the use of the original stand structure.

The performance of both CASTANEA and PDG-Arena at predicting the variability of fir stands productivity remained poor ($r^2 < 13\%$). This can possibly be explained by the presence of three fir stands from the Bauges site that showed particularly large measured growth, a pattern that was not predicted by the models (see Figures B.5 and B.6). The mismatch could result from the time elapsed between the year of measured growth (1996-2013) and the year of measurement of the Leaf Area Index (2022 for the Bauges site), that drives CASTANEA physiological processes. The value of LAI we measured reflects recent extreme hot and dry events (Rakovec et al., 2022) that the growth data necessarily did not capture.

Interestingly, a positive and significant net biodiversity effect was observed in PDG-Arena simulations on gross primary productivity by comparing simulations with interacting species to equivalent simulations with species in isolation. The simulated overyielding can be attributed to an improvement of canopy absorbance due to species mixing (Figure 4). Leaf area being equal between each simulation modality for the same stand, the increased light absorption is explained by a greater occupation of the aerial space in mixed stands, an effect known as canopy packing and that has been observed on a variety of mixed forests across Europe

(Jucker et al., 2015; Pretzsch, 2019). Here, the mixing effect was tested on regularized inventories, which means that trees had the same diameter per species and were regularly spaced. Therefore, only vertical stratification, and no crown plasticity could emerge in the simulation Jucker et al. (2015).

In addition, species mixing increased the yearly water shortage, due to increased transpiration (Figure B.7). This confirms the idea that the nature of the diversity-functioning relationship in forests strongly depends on the limiting resources (Forrester, 2014). According to our simulations, promoting diverse stands could maximize light interception Jucker et al. (2015) but would also increase transpiration, which would be detrimental in water-stressed sites. The use of an individual-based and process-based model such as PDG-Arena, in combination with the measurements of physiological traits in mixed stands could help better understand the relationship between tree diversity, stand productivity and resistance to water stress.

One limit of this study was the nature of the data used to evaluate the model. Tree growth is an integrative measure that results from carbon, water and light uptake, whereas CASTANEA is calibrated using CO_2 fluxes, (Dufrêne et al., 2005). Moreover, the modeling of carbon allocation, which plays a decisive role in simulating wood growth, can still be improved (Davi et al., 2009; Merganičová et al., 2019). Additionally, the climate was parameterized at the site scale instead of the stand scale, although climatic variables such as precipitation could vary between stands due to local topography.

PDG-Arena can be developed further for simulating even more finely interspecific interactions. Firstly, the modeling of the soil does not let individual trees uptake water from different sources whether horizontally or vertically, although

this has been proven to occur and be a factor of species differentiation (Schume et al., 2004). Although in our case, the distribution of trees over a small area (a few meters) may allow us to neglect horizontal heterogeneity, an effort should be made to differentiate access to the soil water resource according to the state of the trees (age, size) but also according to interspecific differences. Secondly, we did not implement phenotypic plasticity, which plays a significant role in the functioning of mixed forests (Pretzsch, 2019; Dieler and Pretzsch, 2013; Jucker et al., 2015). Thus, our model can only simulate the vertical stratification of crowns, but not their morphological adaptation to their local competitor (see, for example, Jonard et al., 2020 and Morin et al., 2021). Finally, the radiative model of PDG-Arena does not directly simulate intra-annual variation in light competition, which could be caused by species differences in leaf phenology.

In conclusion, the new individual-based model PDG-Arena we developed can accurately simulate the interactions between trees in monospecific and mixed stands and predict their productivity. Compared to CASTANEA, PDG-Arena showed improved predictive capability for beech and mixed beech-fir forests. As PDG-Arena simulates the competition for water and light between trees with no preconceived ideas about the direction of interspecific interaction (from competition to complementarity), it can be used to test specific hypotheses about mixed forests and better understand the diversity-functioning relationship in forests under contrasted scenarios. For example, one could explore the following outstanding questions, keeping in mind that the answers are largely dependent on the species identities (Ratcliffe et al., 2015) and on each resource scarcity in a given environment (Forrester et al., 2017a): is overyielding more likely to occur in less productive sites? (Toïgo et al., 2015) Can overyielding increase water stress in

mixed stands? (Forrester et al., 2016) Lastly, being made on the basis of a physio-demo-genetics model, PDG-Arena is suitable to evaluate the evolutionary dynamics of functional traits under various biotic (stand composition, density and structure) and abiotic (soil, climate) constraints, as intraspecific diversity is a major adaptive force in natural tree populations (Lefèvre et al., 2014; Oddou-Muratorio et al., 2020).

5. Declarations

5.1. Declaration of competing interest

The authors of this publication declare that they have no conflicts of interest.

5.2. Funding source

This work was financed by ADEME, the French Agency for Ecological Transition, and ONF, the French National Forests Office. The observation design used in this study is part of the GMAP network https://oreme.org/observation/foret/gmap/, partly funded by the OSU OREME.

5.3. Credits

Figures 1 and 2 were designed using images from flaticon.com.

5.4. Author contributions

Camille Rouet: Conceptualization, Methodology, Software, Visualization, Writing - Original Draft. **Hendrik Davi**: Conceptualization, Supervision. **Arsène Druel**: Methodology, Writing - Review. **Bruno Fady**: Project administration, Supervision, Writing - Review. **Xavier Morin**: Methodology, Data Curation, Supervision, Writing - Review.

Appendix A. Supplementary description of PDG-Arena

Appendix A.1. Computing of Leaf Mass per Area

The Leaf Mass per Area (LMA) is a key physiological parameter defining the mass per unit area of leaves (g/m^2). LMA varies both in time during leaf growth and in space: leaf mass gain is indeed favored by the light level, resulting in an exponentially decreasing distribution of LMA across the canopy from top to bottom. In the CASTANEA model, which assumes that the stand is homogeneous and monospecific, the LMA decay follows an exponential distribution according to an attenuation coefficient $kLMA$ for each species:

$$LMA(LAI_{above}) = LMA_0 \times e^{kLMA \times LAI_{above}} \tag{A.1}$$

LAI_{above} is given by the position of the considered layer within the canopy. The average LMA within a layer is then obtained by integrating $LMA(LAI_{above})$ within the layer vertical boundaries. LMA_0 and $kLMA$ depend on the species and describe the decrease in LMA within the canopy, which itself depends on the decrease in light intensity within the canopy.

In the case of the PDG-Arena model, the canopy is more structurally complex than in CASTANEA and can include several species with different k_{LMA}. Then, the LMA of each crown is defined according to its position within the global canopy, taking all trees into account and using the same equation as A.1. Here, LAI_{above} is computed as the sum of the LAI from the different crowns that are located above the considered layer of leaves. It should be noted that the model is not completely accurate given that the parameter $kLMA$ is species-dependent, although the leaves taken into account in LAI_{above} potentially come

from another species. However, this method does represent the phenomenon of light attenuation which is specific to each individual.

Appendix A.2. Estimation of the attenuation coefficient with reverse-engineering

In order to know the value of the attenuation coefficients of each species in PDG-Arena, a preliminary simulation is carried out following the CASTANEA model to take advantage of the SAIL, its radiation balance sub-model (Dufrêne et al., 2005). The preliminary simulation is performed for each species on a monospecific and regularized inventory (RN inventory, see section 2.3). We define the attenuation coefficient k_1 at a given time as a function of the incident energy I_0, the energy transmitted by the vegetation I_t, and the Leaf Area Index LAI, following a Beer-Lambert model:

$$I_t = I_0 exp^{-k_1 \times LAI} \tag{A.2}$$

which is equivalent to:

$$k_1 = \frac{1}{LAI} \times log(\frac{I_0}{I_t}) \tag{A.3}$$

where I_t is defined at any time as the difference between the incident energy and the energy absorbed by the vegetation.

The coefficient of attenuation which is used in SamsaraLight, denoted k_2, is not of the same nature as k_1. Indeed, in equation A.2, we multiply k_1 to the LAI (considering an infinite, horizontally homogeneous, leaf layer) while SamsaraLight multiplies k_2 to the Leaf Area Density LAD and the beam path length within a finite, volumetric crown (see equation 2). Then, to go from one to the other, we must multiply k_1 by $sin(\beta)$ (with β the angle of height of the

sun):

$$k_2 = sin(\beta) \times k_1 = sin(\beta) \times \frac{1}{LAI} \times log(\frac{I_0}{I_t}) \tag{A.4}$$

The coefficient k_2 depends on the height of the sun, but also on the frequency domain of the radiation. Indeed, the attenuation coefficient takes into account both the extinction of the rays (defined by the leaf and crown geometry) and the absorption by the leaves which depends on the light frequency. In the following calculations, we distinguish the PAR (photosynthetically active radiations) domain for which the absorption is maximized and the NIR (near infrared radiations) domain. It is assumed that these two domains represent the bulk of the incident radiation. To sum up, the attenuation coefficient depends on the species (leaf angle distribution and absorbance rate), the type of radiation (PAR/NIR, direct/diffuse) and the height angle (β).

Based on the results of the preliminary CASTANEA simulation, which executes a radiation balance using the SAIL model, we infer the value of the attenuation coefficients of the plot for direct and diffuse radiations. In the preliminary simulation, we know for direct rays the value of the height angle β at any hour. For diffuse rays, by definition β takes every value between 0 and $\pi/2$ at any hour, so we can't use the height angle information.

Direct Rays.

For direct radiation, we estimate an attenuation coefficient for each species by discriminating the PAR and NIR and defining 20 classes of attenuation coefficient corresponding to classes of height angle β, equally distributed between 0 and $\pi/2$. For each i class of β, we performed an average on the attenuation coefficients

observed during the preliminary simulation for direct radiations:

$$k_{dir}(i) = \sum_{h_i} \left[sin(\beta(h_i)) \times \frac{1}{LAI(h_i)} \times log\left(\frac{I_{0dir}(h_i)}{I_{tdir}(h_i)}\right) \right] \times \frac{1}{n(h_i)} \qquad \text{(A.5)}$$

$k_{dir}(i)$ is the mean attenuation coefficient computed from the preliminary simulation results, for direct radiation of the height angle class i (which includes $n(h_i)$ hours). For a given hour of the year h_i and sun angle $\beta(h_i)$, $LAI(h_i)$ is the daily Leaf Area Index of the plot, $I_{0dir}(h_i)$, the incident direct energy and $I_{tdir}(h_i)$ is the direct energy transmitted through canopy.

Diffuse Radiation.

For diffuse radiation, we discriminate the attenuation coefficient according to the species and radiation domain only. The attenuation coefficient for diffuse light k_{dif} is assumed to be constant for any sun height angle. To switch from one formulation of the Beer-Lambert law to the other (equation A.4), a value of β is nevertheless needed. We note that the distribution of the diffuse rays along the β height angles is uniform. Then, we use $\overline{sin(\beta)}$, the average of $sin(\beta)$ for β going from 0 to $\pi/2$ (which is about 0.637). For a species and a radiative domain, we compute an average on every day of year of the observed attenuation coefficient during the preliminary simulation:

$$k_{dif} = \sum_{j} \left[\overline{sin(\beta)} \times \frac{1}{LAI(j)} \times log\left(\frac{I_{0dif}(j)}{I_{tdif}(j)}\right) \right] \times \frac{1}{365} \qquad \text{(A.6)}$$

with, for the day j, $LAI(j)$ the Leaf Area Index, $I_{0dif}(j)$ the incident diffuse energy and $I_{tdif}(j)$ is the diffuse energy transmitted through canopy.

Appendix A.3. Distribution of radiations into canopy layers and into sun and shade leaves

In CASTANEA, the energy absorbed by the canopy is distributed into five layers of leaves, which are themselves divided into leaves in direct light (called sun leaves) and leaves in the shade. We present here how PDG-Arena operates the distribution of the absorbed energy by individual crowns.

Proportion of sun leaves of a tree.

The proportion of sun leaves of a crown, i.e., of its leaves subjected to direct radiation, is given by a formula borrowed from the HETEROFOR model (Jonard et al., 2020). Two factors define the shading received by the leaves of a tree: on the one hand, the external shading provided by the competing trees, given by the proportion $pSun_{ext}$; on the other hand, the internal shading provided by the own leaves of a tree, given by the proportion $pSun_{int}$.

The shading provided by the competitors is given by the ratio of the direct energy incident on the tree $I_{d0}(aboveTree)$ to the direct energy incident on the stand $I_{d0}(aboveCanopy)$:

$$pSun_{ext} = \frac{I_{d0}(aboveTree)}{I_{d0}(aboveCanopy)} \tag{A.7}$$

The second quotient to be evaluated is the proportion of the tree's leaves shaded by its own leaves. The shading by the leaves of the tree itself follows the same evolution as the direct radiation within the tree, that is to say a Beer-Lambert law:

$$pSun(l) = p(0) \times exp^{-k_{dir}l} \tag{A.8}$$

where $pSun(l)$ is the proportion of sun leaves remaining after the radiation

passes through the crown, with l the cumulative LAI encountered by the passing beam and k_{dir} the tree extinction coefficient for direct PAR. $p(0) = 1$ is the proportion of sun leaves at the crown entrance ignoring leaves shaded by neighboring trees.

We can compute $LAI_{sun-int}$, the amount of leaves that are not shaded by leaves of the same tree. To do this, we need to integrate $p(l)$ for l ranging from 0 to LAI, the Leaf Area Index of the tree:

$$\begin{aligned} LAI_{sun-int} &= \int_0^{LAI} p(l)dl \\ &= \int_0^{LAI} e^{-k_{dir}l}dl \\ &= \left[\frac{e^{-k_{dir}l}}{-k_{dir}}\right]_0^{LAI} \\ &= \frac{1 - e^{-k_{dir}LAI}}{k_{dir}} \end{aligned} \tag{A.9}$$

Thus, $pSun_{int} = LAI_{sun-int}/LAI$ represents the proportion of leaf remaining in the light when shaded by the tree's own leaves.

Finally, the proportion of sun leaves of a tree is $pSun_{tree} = pSun_{ext} \times pSun_{int}$.

Distribution of radiations by layer.

If SamsaraLight allows us to know the amount of energy absorbed per tree according to each domain (PAR/NIR) and type of energy (direct/diffused), noted E_{tree}, it does not allow us to distribute this amount between layers, differentiating leaves with high interception and leaves with low interception. Firstly, we divide the leaf surface of a tree in n equal-sized layers, and we assume that the radiative

characteristics are homogeneous within a layer. We define a distribution function f_i, that determines E_i, the amount of energy that is absorbed from layer i:

$$E_i = E_{tree} \times \frac{f_i}{\sum_n f_i} \tag{A.10}$$

We assume that the distribution f_i is affected by the light interception from leaf surface that is located above the layer (whether it belongs to other trees or to the same tree). Then, we define a simple stand-scale model that describes the level of energy transmitted through the stand using a Beer-Lambert law. At any level of height located under a quantity of leaves LAI_{above}, the proportion of light transmitted through these leaves is:

$$p_{light}(LAI_{above}) = e^{-k_{st} \times LAI_{above}} \tag{A.11}$$

with k_{st} the stand level attenuation coefficient. LAI_{above} is calculated by counting the amount of leaves above the leaf layer under consideration, knowing the position and shape of each individual. A homogeneous distribution of leaf density within each individual crown is assumed. We do not consider the slope in this calculation, i.e., only the height of the trees defines whether the leaves of one tree are higher than those of another.

Finally, to calculate f_i, the fraction of energy absorbed by any layer i of a crown, we compute the average value of p_{light} inside the layer by integrating it within its boundaries $LAI_{above}(i-1)$ and $LAI_{above}(i)$:

$$
\begin{aligned}
f_i &= \frac{\int_{LAI_{above}(i-1)}^{LAI_{above}(i)} e^{-k_{st} LAI_{above}} dLAI_{above}}{LAI_{above}(i) - LAI_{above}(i-1)} \\
&\iff \\
f_i &= \frac{e^{-k_{st} LAI_{above}(i-1)} - e^{-k_{st} LAI_{above}(i)}}{k_{st}(LAI_{above}(i) - LAI_{above}(i-1))}
\end{aligned}
\tag{A.12}
$$

The proportion f_i is computed for each type of radiation (direct/diffuse and PAR/NIR).

Appendix A.4. Reduction of absorbed radiations in SamsaraLight

In SamsaraLight standard mode, the foliage is assumed to be at its maximum during the whole process. Thus, the energy absorbed by the trees when their leaf area is in reality lower must be revised downwards, especially for deciduous trees, which lose all their foliage in autumn. For each individual, a ratio depending on its LAI is computed each day to represent the evolution of its absorption level from 0 to 1. The level of absorption is supposed to follow the dynamic of the Beer-Lambert law:

$$
ratio_{LAI} = \frac{1 - e^{-k \times LAI}}{1 - e^{-k \times LAI_{max}}} \tag{A.13}
$$

For each radiation domain, k is the attenuation coefficient of a tree and $ratio_{LAI}$ is applied to its absorbed energy to take off the surplus. Nevertheless, the removed energy must be redistributed, because if it had not been intercepted, this energy would have been distributed among the other absorbing elements (crowns or soil cells). At this point, it is no longer possible to know to which element the energy should be distributed. Then, the extracted energy is

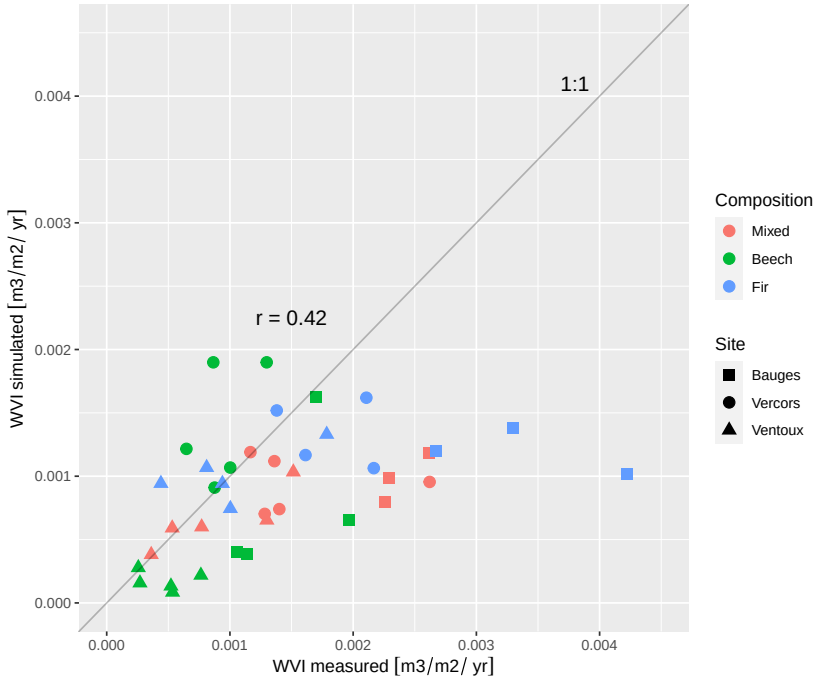

Figure B.5: Simulated versus measured Wood Volume Increment per stand for the CASTANEA model. r is the correlation coefficient.

redistributed to all absorbing elements, proportionally to their level of absorbed energy (after reduction according to LAI), which represents their relative interception capacity.

Appendix B. Supplementary figures

Figures B.5 and B.6 show the simulated versus measured wood volume increment per stand for the 39 stands using the CASTANEA model and the PDG-Arena model (with O inventories), respectively.

Figure B.7 shows the maximum water shortage during an average year (i.e. the maximum difference reached during a year between the current and full useful reserve, in mm) and yearly transpiration simulated by PDG-Arena for 13 mixed

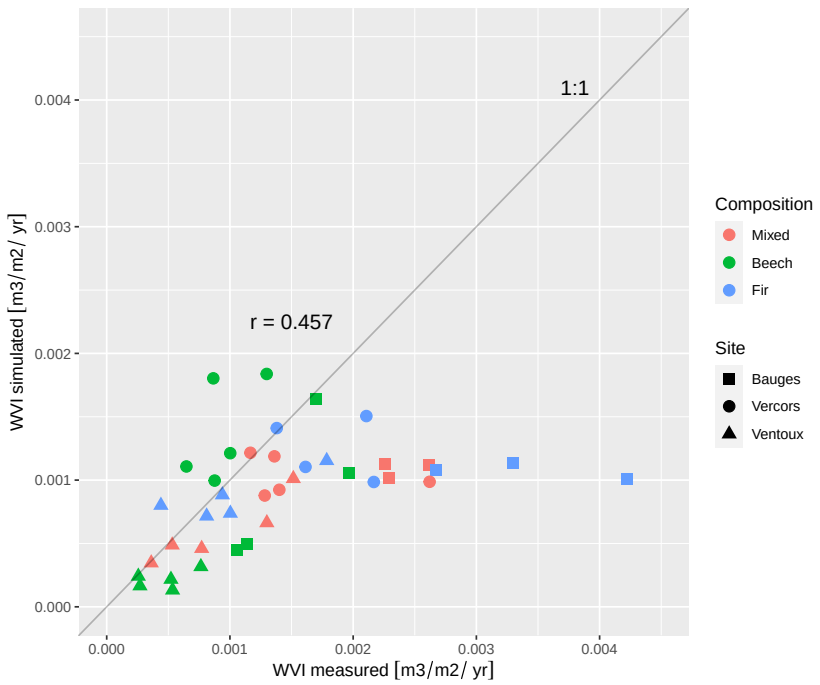

Figure B.6: Simulated versus measured Wood Volume Increment per stand for the PDG-Arena model using original inventories. r is the correlation coefficient.

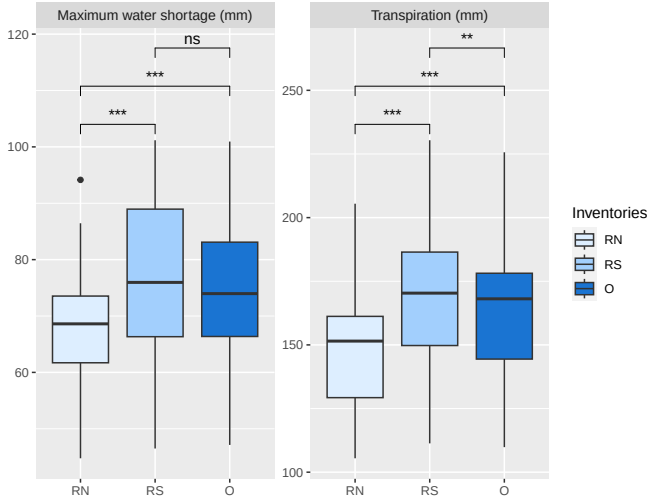

Figure B.7: Maximum water shortage during an average year and yearly transpiration simulated by PDG-Arena for 13 mixed stands.Three types of inventories were used: regularized inventories with no species interactions (RN), regularized inventories with species interactions (RS) and original inventories (O). Two-sided Wilcoxon signed rank test was used (***: p-value < 0.001).

stands using RN, RS and O inventories.

References

Ammer, C., 2019. Diversity and forest productivity in a changing climate. New Phytologist 221, 50–66. doi:10.1111/nph.15263.

Bauhus, J., Forrester, D.I., Pretzsch, H., 2017. From Observations to Evidence About Effects of Mixed-Species Stands, in: Pretzsch, H., Forrester, D.I., Bauhus, J. (Eds.), Mixed-Species Forests: Ecology and Management. Springer, Berlin, Heidelberg, pp. 27–71. doi:10.1007/978-3-662-54553-9_2.

Bonan, G.B., 2008. Forests and Climate Change: Forcings, Feedbacks, and the Climate Benefits of Forests. Science 320, 1444–1449. doi:10.1126/science.1155121.

Cordonnier, T., Smadi, C., Kunstler, G., Courbaud, B., 2019. Asymmetric competition, ontogenetic growth and size inequality drive the difference in productivity between two-strata and one-stratum forest stands. Theoretical Population Biology 130, 83–93. doi:10.1016/j.tpb.2019.07.001.

Courbaud, B., de Coligny, F., Cordonnier, T., 2003. Simulating radiation distribution in a heterogeneous Norway spruce forest on a slope. Agricultural and Forest Meteorology 116, 1–18. doi:10.1016/S0168-1923(02)00254-X.

Cuddington, K., Fortin, M.J., Gerber, L.R., Hastings, A., Liebhold, A., O'Connor, M., Ray, C., 2013. Process-based models are required to manage ecological systems in a changing world. Ecosphere 4, art20. doi:10.1890/ES12-00178.1.

Davi, H., Barbaroux, C., Dufrêne, E., François, C., Montpied, P., Bréda, N., Badeck, F., 2008a. Modelling leaf mass per area in forest canopy as affected by prevailing radiation conditions. Ecological Modelling 211, 339–349. doi:10.1016/j.ecolmodel.2007.09.012.

Davi, H., Barbaroux, C., Francois, C., Dufrêne, E., 2009. The fundamental role of reserves and hydraulic constraints in predicting LAI and carbon allocation in forests. Agricultural and Forest Meteorology 149, 349–361. doi:10.1016/j.agrformet.2008.08.014.

Davi, H., Baret, F., Huc, R., Dufrêne, E., 2008b. Effect of thinning on LAI variance in heterogeneous forests. Forest Ecology and Management 256, 890–899. doi:10.1016/j.foreco.2008.05.047.

Davi, H., Cailleret, M., 2017. Assessing drought-driven mortality trees with physiological process-based models. Agricultural and Forest Meteorology 232, 279–290. doi:10.1016/j.agrformet.2016.08.019.

Dieler, J., Pretzsch, H., 2013. Morphological plasticity of European beech (Fagus sylvatica L.) in pure and mixed-species stands. Forest Ecology and Management 295, 97–108. doi:10.1016/j.foreco.2012.12.049.

Dufour-Kowalski, S., Courbaud, B., Dreyfus, P., Meredieu, C., de Coligny, F., 2012. Capsis: an open software framework and community for forest growth modelling. Annals of Forest Science 69, 221–233. doi:10.1007/s13595-011-0140-9.

Dufrêne, E., Davi, H., François, C., Maire, G.l., Dantec, V.L., Granier, A., 2005. Modelling carbon and water cycles in a beech forest. Part I: Model description and uncertainty analysis on modelled NEE. Ecological Modelling 185, 407–436. doi:10/fjnfgr.

Dănescu, A., Albrecht, A.T., Bauhus, J., 2016. Structural diversity promotes productivity of mixed, uneven-aged forests in southwestern Germany. Oecologia 182, 319–333. doi:10.1007/s00442-016-3623-4.

Fontes, L., Bontemps, J.D., Bugmann, H., Oijen, M.v., Gracia, C., Kramer, K., Lindner, M., Rötzer, T., Skovsgaard, J.P., 2010. Models for supporting forest management in a changing environment. Forest Systems 19, 8–29.

Forrester, D.I., 2014. The spatial and temporal dynamics of species interactions in mixed-species forests: From pattern to process. Forest Ecology and Management 312, 282–292. doi:10.1016/j.foreco.2013.10.003.

Forrester, D.I., Ammer, C., Annighöfer, P.J., Avdagic, A., Barbeito, I., Bielak, K., Brazaitis, G., Coll, L., del Río, M., Drössler, L., Heym, M., Hurt, V., Löf, M., Matović, B., Meloni, F., den Ouden, J., Pach, M., Pereira, M.G., Ponette, Q., Pretzsch, H., Skrzyszewski, J., Stojanović, D., Svoboda, M., Ruiz-Peinado, R., Vacchiano, G., Verheyen, K., Zlatanov, T., Bravo-Oviedo, A., 2017a. Predicting the spatial and temporal dynamics of species interactions in Fagus sylvatica and Pinus sylvestris forests across Europe. Forest Ecology and Management 405, 112–133. doi:10.1016/j.foreco.2017.09.029.

Forrester, D.I., Bauhus, J., 2016. A Review of Processes Behind Diversity—Productivity Relationships in Forests. Current Forestry Reports 2, 45–61. doi:10.1007/s40725-016-0031-2.

Forrester, D.I., Bonal, D., Dawud, S., Gessler, A., Granier, A., Pollastrini, M., Grossiord, C., 2016. Drought responses by individual tree species are not often correlated with tree species diversity in European forests. Journal of Applied Ecology 53, 1725–1734. doi:10.1111/1365-2664.12745.

Forrester, D.I., Tachauer, I.H.H., Annighoefer, P., Barbeito, I., Pretzsch, H., Ruiz-Peinado, R., Stark, H., Vacchiano, G., Zlatanov, T., Chakraborty, T., Saha, S., Sileshi, G.W., 2017b. Generalized biomass and leaf area allometric equations for European tree species incorporating stand structure, tree age and climate. Forest Ecology and Management 396, 160–175. doi:10.1016/j.foreco.2017.04.011.

Gonçalves, A.F.A., Santos, J.A.d., França, L.C.d.J., Campoe, O.C., Altoé, T.F., Scolforo, J.R.S., 2021. Use of the process-based models in forest research: a bibliometric review. CERNE 27, e. doi:10.1590/01047760202127012769.

Grossiord, C., 2018. Having the right neighbors: how tree species diversity modulates drought impacts on forests. New Phytologist 228, 42–49. doi:https://doi.org/10.1111/nph.15667.

Grossiord, C., Granier, A., Ratcliffe, S., Bouriaud, O., Bruelheide, H., Chećko, E., Forrester, D.I., Dawud, S.M., Finér, L., Pollastrini, M., Scherer-Lorenzen, M., Valladares, F., Bonal, D., Gessler, A., 2014. Tree diversity does not always improve resistance of forest ecosystems to drought. Proceedings of the National Academy of Sciences 111, 14812–14815. doi:10.1073/pnas.1411970111.

Guillemot, J., Kunz, M., Schnabel, F., Fichtner, A., Madsen, C.P., Gebauer, T., Härdtle, W., von Oheimb, G., Potvin, C., 2020. Neighbourhood-mediated shifts in tree biomass allocation drive overyielding in tropical species mixtures. New Phytologist 228, 1256–1268. doi:10.1111/nph.16722.

Jonard, M., André, F., de Coligny, F., de Wergifosse, L., Beudez, N., Davi, H., Ligot, G., Ponette, Q., Vincke, C., 2020. HETEROFOR 1.0: a spatially explicit model for exploring the response of structurally complex forests to uncertain future conditions – Part 1: Carbon fluxes and tree dimensional growth. Geoscientific Model Development 13, 905–935. doi:10.5194/gmd-13-905-2020.

Jourdan, M., Cordonnier, T., Dreyfus, P., Riond, C., de Coligny, F., Morin, X., 2021. Managing mixed stands can mitigate severe climate change impacts on French alpine forests. Regional Environmental Change 21, 78. doi:10.1007/s10113-021-01805-y.

Jourdan, M., Kunstler, G., Morin, X., 2020. How neighbourhood interactions control the temporal stability and resilience to drought of trees in mountain forests. Journal of Ecology 108, 666–677. doi:https://doi.org/10.1111/1365-2745.13294.

Jourdan, M., Lebourgeois, F., Morin, X., 2019. The effect of tree diversity on the resistance and recovery of forest stands in the French Alps may depend on species differences in hydraulic features. Forest Ecology and Management 450, 117486. doi:10.1016/j.foreco.2019.117486.

Jucker, T., Bouriaud, O., Avacaritei, D., Dănilă, I., Duduman, G., Valladares, F., Coomes, D.A., 2014. Competition for light and water play contrasting roles in driving diversity-productivity relationships in Iberian forests. Journal of Ecology 102, 1202–1213. doi:10.1111/1365-2745.12276.

Jucker, T., Bouriaud, O., Coomes, D.A., 2015. Crown plasticity enables trees to optimize canopy packing in mixed-species forests. Functional Ecology 29, 1078–1086. doi:10.1111/1365-2435.12428.

Korzukhin, M.D., Ter-Mikaelian, M.T., Wagner, R.G., 1996. Process versus empirical models: which approach for forest ecosystem management? Canadian Journal of Forest Research 26, 879–887. doi:10.1139/x26-096.

Lefèvre, F., Boivin, T., Bontemps, A., Courbet, F., Davi, H., Durand-Gillmann, M., Fady, B., Gauzere, J., Gidoin, C., Karam, M.J., Lalagüe, H., Oddou-Muratorio, S., Pichot, C., 2014. Considering evolutionary processes in adaptive forestry. Annals of Forest Science 71, 723–739. doi:10.1007/s13595-013-0272-1.

Leuning, R., Kelliher, F.M., Pury, D.G.G.D., Schulze, E.D., 1995. Leaf nitrogen, photosynthesis, conductance and transpiration: scaling from leaves to canopies. Plant, Cell & Environment 18, 1183–1200. doi:https://doi.org/10.1111/j.1365-3040.1995.tb00628.x.

Liang, J., Crowther, T.W., Picard, N., Wiser, S., Zhou, M., Alberti, G., Schulze, E.D., McGuire, A.D., Bozzato, F., Pretzsch, H., de Miguel, S., Paquette, A., Hérault, B., Scherer-Lorenzen, M., Barrett, C.B., Glick, H.B., Hengeveld, G.M., Nabuurs, G.J., Pfautsch, S., Viana, H., Vibrans, A.C., Ammer, C., Schall, P., Verbyla, D., Tchebakova, N., Fischer, M., Watson, J.V., Chen, H.Y.H., Lei, X., Schelhaas, M.J., Lu, H., Gianelle, D., Parfenova, E.I., Salas, C., Lee, E., Lee, B., Kim, H.S., Bruelheide, H., Coomes, D.A., Piotto, D., Sunderland, T., Schmid, B., Gourlet-Fleury, S., Sonké, B., Tavani, R., Zhu, J., Brandl, S., Vayreda, J., Kitahara, F., Searle, E.B., Neldner, V.J., Ngugi, M.R., Baraloto, C., Frizzera, L., Bałazy, R., Oleksyn, J., Zawiła-Niedźwiecki, T., Bouriaud, O., Bussotti, F., Finér, L., Jaroszewicz, B., Jucker, T., Valladares, F., Jagodzinski, A.M., Peri, P.L., Gonmadje, C., Marthy, W., O'Brien, T., Martin, E.H., Marshall, A.R., Rovero, F., Bitariho, R., Niklaus, P.A., Alvarez-Loayza, P., Chamuya, N., Valencia, R., Mortier, F., Wortel, V., Engone-Obiang, N.L., Ferreira, L.V., Odeke, D.E., Vasquez, R.M., Lewis, S.L., Reich, P.B.,

2016. Positive biodiversity-productivity relationship predominant in global forests. Science 354. doi:10.1126/science.aaf8957.

Lindner, M., Maroschek, M., Netherer, S., Kremer, A., Barbati, A., Garcia-Gonzalo, J., Seidl, R., Delzon, S., Corona, P., Kolström, M., Lexer, M.J., Marchetti, M., 2010. Climate change impacts, adaptive capacity, and vulnerability of European forest ecosystems. Forest Ecology and Management 259, 698–709. doi:10.1016/j.foreco.2009.09.023.

Loreau, M., 2010. CHAPTER 3. Biodiversity and Ecosystem Functioning, in: From Populations to Ecosystems. Princeton University Press, pp. 56–78. doi:10.1515/9781400834167.56.

Mas, E., Cochard, H., Deluigi, J., Didion-Gency, M., Martin-StPaul, N., Morcillo, L., Valladares, F., Vilagrosa, A., Grossiord, C., 2024. Interactions between beech and oak seedlings can modify the effects of hotter droughts and the onset of hydraulic failure. New Phytologist 241, 1021–1034. doi:10.1111/nph.19358.

Merganičová, K., Merganič, J., Lehtonen, A., Vacchiano, G., Sever, M.Z.O., Augustynczik, A.L.D., Grote, R., Kyselová, I., Mäkelä, A., Yousefpour, R., Krejza, J., Collalti, A., Reyer, C.P.O., 2019. Forest carbon allocation modelling under climate change. Tree Physiology 39, 1937–1960. doi:10/ghkr6m.

Messier, C., Bauhus, J., Sousa-Silva, R., Auge, H., Baeten, L., Barsoum, N., Bruelheide, H., Caldwell, B., Cavender-Bares, J., Dhiedt, E., Eisenhauer, N., Ganade, G., Gravel, D., Guillemot, J., Hall, J.S., Hector, A., Hérault, B., Jactel, H., Koricheva, J., Kreft, H., Mereu, S., Muys, B., Nock, C.A., Paquette, A., Parker, J.D., Perring, M.P., Ponette, Q., Potvin, C., Reich, P.B., Scherer-Lorenzen, M., Schnabel, F., Verheyen, K., Weih, M., Wollni, M., Zemp, D.C., 2022. For the sake of resilience and multifunctionality, let's diversify planted forests! Conservation Letters 15, e12829. doi:10.1111/conl.12829.

Metz, J., Annighöfer, P., Schall, P., Zimmermann, J., Kahl, T., Schulze, E.D., Ammer, C., 2016. Site-adapted admixed tree species reduce drought susceptibility of mature European beech. Global Change Biology 22, 903–920. doi:10.1111/gcb.13113.

Monteith, J., 1965. Evaporation and environment. Symposia of the Society for Experimental Biology .

Morin, X., Bugmann, H., de Coligny, F., Martin-StPaul, N., Cailleret, M., Limousin, J.M., Ourcival, J.M., Prevosto, B., Simioni, G., Toigo, M., Vennetier, M., Catteau,

E., Guillemot, J., 2021. Beyond forest succession: A gap model to study ecosystem functioning and tree community composition under climate change. Functional Ecology 35, 955–975. doi:10.1111/1365-2435.13760.

Morin, X., Fahse, L., de Mazancourt, C., Scherer-Lorenzen, M., Bugmann, H., 2014. Temporal stability in forest productivity increases with tree diversity due to asynchrony in species dynamics. Ecology Letters 17, 1526–1535. doi:10.1111/ele.12357.

Morin, X., Fahse, L., Scherer-Lorenzen, M., Bugmann, H., 2011. Tree species richness promotes productivity in temperate forests through strong complementarity between species: Species richness promotes forest productivity. Ecology Letters 14, 1211–1219. doi:10.1111/j.1461-0248.2011.01691.x.

Oddou-Muratorio, S., Davi, H., Lefèvre, F., 2020. Integrating evolutionary, demographic and ecophysiological processes to predict the adaptive dynamics of forest tree populations under global change. Tree Genetics & Genomes 16, 67. doi:10.1007/s11295-020-01451-1.

Oddou-Muratorio, S., Davi, H., 2014. Simulating local adaptation to climate of forest trees with a Physio-Demo-Genetics model. Evolutionary Applications 7, 453–467. doi:10.1111/eva.12143.

Pardos, M., del Río, M., Pretzsch, H., Jactel, H., Bielak, K., Bravo, F., Brazaitis, G., Defossez, E., Engel, M., Godvod, K., Jacobs, K., Jansone, L., Jansons, A., Morin, X., Nothdurft, A., Oreti, L., Ponette, Q., Pach, M., Riofrío, J., Ruíz-Peinado, R., Tomao, A., Uhl, E., Calama, R., 2021. The greater resilience of mixed forests to drought mainly depends on their composition: Analysis along a climate gradient across Europe. Forest Ecology and Management 481, 118687. doi:10.1016/j.foreco.2020.118687.

Piotto, D., 2008. A meta-analysis comparing tree growth in monocultures and mixed plantations. Forest Ecology and Management 255, 781–786. doi:10.1016/j.foreco.2007.09.065.

van der Plas, F., Manning, P., Allan, E., Scherer-Lorenzen, M., Verheyen, K., Wirth, C., Zavala, M.A., Hector, A., Ampoorter, E., Baeten, L., Barbaro, L., Bauhus, J., Benavides, R., Benneter, A., Berthold, F., Bonal, D., Bouriaud, O., Bruelheide, H., Bussotti, F., Carnol, M., Castagneyrol, B., Charbonnier, Y., Coomes, D., Coppi, A., Bastias, C.C., Muhie Dawud, S., De Wandeler, H., Domisch, T., Finér, L., Gessler, A., Granier, A., Grossiord, C., Guyot, V., Hättenschwiler, S., Jactel, H., Jaroszewicz, B., Joly, F.X., Jucker, T., Koricheva, J., Milligan, H., Müller, S., Muys,

B., Nguyen, D., Pollastrini, M., Raulund-Rasmussen, K., Selvi, F., Stenlid, J., Valladares, F., Vesterdal, L., Zielínski, D., Fischer, M., 2016. Jack-of-all-trades effects drive biodiversity–ecosystem multifunctionality relationships in European forests. Nature Communications 7, 11109. doi:10.1038/ncomms11109.

Porté, A., Bartelink, H.H., 2002. Modelling mixed forest growth: a review of models for forest management. Ecological Modelling 150, 141–188. doi:10.1016/S0304-3800(01)00476-8.

Pretzsch, H., 2019. The Effect of Tree Crown Allometry on Community Dynamics in Mixed-Species Stands versus Monocultures. A Review and Perspectives for Modeling and Silvicultural Regulation. Forests 10, 810. doi:10.3390/f10090810.

Pretzsch, H., Forrester, D.I., Bauhus, J. (Eds.), 2017. Mixed-species forests : ecology and management. Springer, Berlin.

Pretzsch, H., Forrester, D.I., Rötzer, T., 2015. Representation of species mixing in forest growth models. A review and perspective. Ecological Modelling 313, 276–292. doi:10.1016/j.ecolmodel.2015.06.044.

Pretzsch, H., Schütze, G., Uhl, E., 2013. Resistance of European tree species to drought stress in mixed versus pure forests: evidence of stress release by inter-specific facilitation. Plant Biology 15, 483–495. doi:https://doi.org/10.1111/j.1438-8677.2012.00670.x.

Rakovec, O., Samaniego, L., Hari, V., Markonis, Y., Moravec, V., Thober, S., Hanel, M., Kumar, R., 2022. The 2018–2020 Multi-Year Drought Sets a New Benchmark in Europe. Earth's Future 10, e2021EF002394. doi:10.1029/2021EF002394.

Ratcliffe, S., Holzwarth, F., Nadrowski, K., Levick, S., Wirth, C., 2015. Tree neighbourhood matters – Tree species composition drives diversity–productivity patterns in a near-natural beech forest. Forest Ecology and Management 335, 225–234. doi:10.1016/j.foreco.2014.09.032.

Ratcliffe, S., Liebergesell, M., Ruiz-Benito, P., González, J.M., Castañeda, J.M.M., Kändler, G., Lehtonen, A., Dahlgren, J., Kattge, J., Peñuelas, J., Zavala, M.A., Wirth, C., 2016. Modes of functional biodiversity control on tree productivity across the European continent. Global Ecology and Biogeography 25, 251–262. doi:https://doi.org/10.1111/geb.12406.

Reyer, C., 2015. Forest Productivity Under Environmental Change—a Review of Stand-Scale Modeling Studies. Current Forestry Reports 1, 53–68. doi:10.1007/s40725-015-0009-5.

Rolland, C., 2003. Spatial and Seasonal Variations of Air Temperature Lapse Rates in Alpine Regions. Journal of Climate 16, 1032–1046. doi:10.1175/1520-0442(2003)016<1032:SASVOA>2.0.CO;2.

Rouet, C., 2024. Data from: PDG-Arena: An ecophysiological model for characterizing tree-tree interactions in heterogeneous stands (v1.0.0). Zenodo. doi:10.5281/zenodo.10641151.

del Río, M., Pretzsch, H., Ruiz-Peinado, R., Jactel, H., Coll, L., Löf, M., Aldea, J., Ammer, C., Avdagić, A., Barbeito, I., Bielak, K., Bravo, F., Brazaitis, G., Cerný, J., Collet, C., Condés, S., Drössler, L., Fabrika, M., Heym, M., Holm, S.O., Hylen, G., Jansons, A., Kurylyak, V., Lombardi, F., Matović, B., Metslaid, M., Motta, R., Nord-Larsen, T., Nothdurft, A., den Ouden, J., Pach, M., Pardos, M., Poeydebat, C., Ponette, Q., Pérot, T., Reventlow, D.O.J., Sitko, R., Sramek, V., Steckel, M., Svoboda, M., Verheyen, K., Vospernik, S., Wolff, B., Zlatanov, T., Bravo-Oviedo, A., 2022. Emerging stability of forest productivity by mixing two species buffers temperature destabilizing effect. Journal of Applied Ecology 59, 2730–2741. doi:10.1111/1365-2664.14267.

Schume, H., Jost, G., Hager, H., 2004. Soil water depletion and recharge patterns in mixed and pure forest stands of European beech and Norway spruce. Journal of Hydrology 289, 258–274. doi:10.1016/j.jhydrol.2003.11.036.

Seynave, I., Bailly, A., Balandier, P., Bontemps, J.D., Cailly, P., Cordonnier, T., Deleuze, C., Dhôte, J.F., Ginisty, C., Lebourgeois, F., Merzeau, D., Paillassa, E., Perret, S., Richter, C., Meredieu, C., 2018. GIS Coop: networks of silvicultural trials for supporting forest management under changing environment. Annals of Forest Science 75, 1–20. doi:10.1007/s13595-018-0692-z.

Toïgo, M., Vallet, P., Perot, T., Bontemps, J.D., Piedallu, C., Courbaud, B., 2015. Overyielding in mixed forests decreases with site productivity. Journal of Ecology 103, 502–512. doi:10.1111/1365-2745.12353.

Trogisch, S., Liu, X., Rutten, G., Xue, K., Bauhus, J., Brose, U., Bu, W., Cesarz, S., Chesters, D., Connolly, J., Cui, X., Eisenhauer, N., Guo, L., Haider, S., Härdtle, W., Kunz, M., Liu, L., Ma, Z., Neumann, S., Sang, W., Schuldt, A., Tang, Z., van Dam, N.M., von Oheimb, G., Wang, M.Q., Wang, S., Weinhold, A., Wirth, C., Wubet, T., Xu, X., Yang, B., Zhang, N., Zhu, C.D., Ma, K., Wang, Y., Bruelheide, H., 2021. The significance of tree-tree interactions for forest ecosystem functioning. Basic and Applied Ecology 55, 33–52. doi:10.1016/j.baae.2021.02.003.

Trumbore, S., Brando, P., Hartmann, H., 2015. Forest health and global change. Science 349, 814–818. doi:10.1126/science.aac6759.

Vidal, J.P., Martin, E., Franchistéguy, L., Baillon, M., Soubeyroux, J.M., 2010. A 50-year high-resolution atmospheric reanalysis over France with the Safran system. International Journal of Climatology 30, 1627–1644. doi:10.1002/joc.2003.

Vilà, M., Vayreda, J., Comas, L., Ibáñez, J.J., Mata, T., Obón, B., 2007. Species richness and wood production: a positive association in Mediterranean forests. Ecology Letters 10, 241–250. doi:10.1111/j.1461-0248.2007.01016.x.

Zeller, L., Pretzsch, H., 2019. Effect of forest structure on stand productivity in Central European forests depends on developmental stage and tree species diversity. Forest Ecology and Management 434, 193–204. doi:10.1016/j.foreco.2018.12.024.

Zhang, Y., Chen, H.Y.H., Reich, P.B., 2012. Forest productivity increases with evenness, species richness and trait variation: a global meta-analysis. Journal of Ecology 100, 742–749. doi:10.1111/j.1365-2745.2011.01944.x.